A stable toolkit method in quantum control

2008 J. Phys. A: Math. Theor. 41 362001

(http://iopscience.iop.org/1751-8121/41/36/362001)

IOP FTC
IOP PUBLISHING JOURNAL OF PHYSICS A: MATHEMATICAL AND THEORETICAL
J. Phys. A: Math. Theor. **41** (2008) 362001 (10pp) doi:10.1088/1751-8113/41/36/362001

FAST TRACK COMMUNICATION

A stable toolkit method in quantum control

M Belhadj[1], **J Salomon**[2] **and G Turinici**[2]

[1] Institut Supérieur des Mathématiques Appliquées et d'Informatique de Kairouan, Av. Assad Ibn El Fourat, 3100 Kairouan, Tunisie
[2] CEREMADE, Université Paris Dauphine, Place du Maréchal De Lattre De Tassigny, 75775 Paris Cedex 16, France

E-mail: mohamed.belhadj@ismai.rnu.tn, salomon@ceremade.dauphine.fr and gabriel.turinici@dauphine.fr

Received 8 April 2008
Published 1 August 2008
Online at stacks.iop.org/JPhysA/41/362001

Abstract
Recently the 'toolkit' discretization introduced to accelerate the numerical resolution of the time-dependent Schrödinger equation arising in quantum optimal control problems demonstrated good results on a large range of models. However, when coupling this class of methods with the so-called monotonically convergent algorithms, numerical instabilities affect the convergence of the discretized scheme. We present an adaptation of the 'toolkit' method which preserves the monotonicity of the procedure. The theoretical properties of the new algorithm are illustrated by numerical simulations.

PACS numbers: 32.80, QK

1. Introduction

We introduce in this communication a technique that addresses the numerical resolution of the time-dependent Schrödinger equation (TDSE) in a quantum control framework. The method uses the 'toolkit' method introduced by Rabitz *et al* [1–3] as a numerical solver of TDSE, and the monotonically convergent algorithms [4, 5] as an optimization method to compute optimal electrical fields. However, the monotonicity may be lost after time discretization. The goal of this work is to explain how to conserve it using a toolkit procedure used for time discretization.

Let us briefly present the model and the corresponding optimal control framework used here. Consider a quantum system described by its wavefunction $\Psi(t, x)$. Here x denotes the space variable belonging to $\mathbb{R}^\gamma$ (for some $\gamma \geqslant 1$). The dynamics of this system is characterized by its internal Hamiltonian,

$$H_0 = K + V(x). \tag{1}$$

In this equation K, the kinetic part, could be $-\Delta$ (the Laplacian) while $V(x)$ is the potential operator. By assumption this Hamiltonian does not give rise to an appropriate evolution and

an external interaction is introduced to obtain a desired final state. This interaction is taken here as an electric field with time-dependent amplitude $\varepsilon(t)$ that acts on the system through a time-independent dipole moment operator μ. We obtain the new Hamiltonian $H = H_0 - \mu\varepsilon(t)$ and the corresponding Schrödinger equation (we work in atomic units, i.e. $\hbar = 1$) which reads

$$\text{(TDSE)} \begin{cases} \mathrm{i}\partial_t \Psi(t,x) = H\Psi(t,x) \\ \Psi(t=0,x) = \Psi_{\text{init}}(x), \end{cases} \tag{2}$$

where Ψ_{init} is the initial condition for Ψ subject to the constraint

$$\|\Psi_{\text{init}}\|_{L^2(\mathbb{R}^\nu)} = 1.$$

As H_0 and μ are supposed self-adjoint, the L^2 norm of the state is constant with respect to the time. In numerical simulations, the ground state, i.e. an unitary eigenvector of H_0 associated to the lowest eigenvalue, is generally taken as initial state ψ_{init}.

The optimal control assesses the fitness of the control $\varepsilon(t)$ and of the final state $\Psi(T)$ through the introduction of a functional J to be maximized; this functional includes on the one hand terms that describe the objectives and on the other hand terms that penalize undesired effects. One simple example of a functional is

$$J(\varepsilon) = \langle \Psi(T)|O|\Psi(T)\rangle - \alpha \int_O^T \varepsilon^2(t)\,\mathrm{d}t. \tag{3}$$

Here and in what follows, we use the convention that for any function f and g and any operator A: $\langle f|A|g\rangle = \int_{\mathbb{R}^\nu} \overline{f(x)} Ag(x)\,\mathrm{d}x$. The coefficient α is a positive parameter (it may also depend on time, cf [6]) and O is the observable operator that encodes the goal; the larger the value $\langle \Psi(T)|O|\Psi(T)\rangle$ is, the better the control objectives have been met.

The maximization of the functional J is realized by solving the Euler–Lagrange critical point equations; a standard way to write these equations is to introduce an *adjoint state* $\chi(t,x)$ acting as a Lagrange multiplier. Denoting by $\mathrm{Im}(z)$, the imaginary part of the complex number z, the following critical point equations are obtained [7]:

$$\begin{cases} \mathrm{i}\partial_t \Psi(t,x) = (H_0 - \mu\varepsilon(t))\Psi(t,x), \\ \Psi(t=0,x) = \Psi_{\text{init}}(x), \end{cases} \tag{4}$$

$$\begin{cases} \mathrm{i}\partial_t \chi(t,x) = (H_0 - \mu\varepsilon(t))\chi(t,x), \\ \chi(t=T,x) = O\Psi(T,x), \end{cases} \tag{5}$$

$$\alpha\varepsilon(t) = -\mathrm{Im}\langle \chi|\mu|\Psi\rangle(t). \tag{6}$$

Efficient strategies to solve in practice the system (4)–(6) are given by the monotonically convergent algorithms [7, 8] that are guaranteed to improve the functional J values at each iteration. A general formulation of these monotonic algorithms is given by the following system [4], which have to be solved iteratively at each step,

$$\begin{cases} \mathrm{i}\partial_t \Psi^k(t,x) = (H_0 - \mu\varepsilon^k(t))\Psi^k(t,x), \\ \Psi^k(t=0,x) = \Psi_{\text{init}}(x), \end{cases} \tag{7}$$

$$\varepsilon^k(t) = (1-\delta)\tilde{\varepsilon}^{k-1}(t) - \frac{\delta}{\alpha}\,\mathrm{Im}\langle \chi^{k-1}|\mu|\Psi^k\rangle(t). \tag{8}$$

$$\begin{cases} \mathrm{i}\partial_t \chi^k(t,x) = (H_0 - \mu\tilde{\varepsilon}^k(t))\chi^k(t,x), \\ \chi^k(t=T,x) = O\Psi^k(T,x), \end{cases} \tag{9}$$

$$\tilde{\varepsilon}^k(t) = (1-\eta)\varepsilon^k(t) - \frac{\eta}{\alpha}\,\mathrm{Im}\langle\chi^k|\mu|\Psi^k\rangle(t), \tag{10}$$

where δ and η are two real parameters in $[0, 2]$ with $(\delta, \eta) \neq (0, 0)$.

The most important property of this algorithm is given in the following theorem:

Theorem 1 ([4]). *Suppose O is a self-adjoint positive semi-definite operator. Then, for any $\delta, \eta \in [0, 2]$ the algorithm given in equations (7)–(10) converges monotonically in the sense that $J(\varepsilon^{k+1}) \geqslant J(\varepsilon^k)$.*

In what follows, we show how to adapt this algorithm to the toolkit method. The communication is organized as follows: in section 2, we introduce the discrete setting of our optimization problem. The toolkit methods together with the monotonic schemes are described in section 3. The definition of our algorithm is given in section 4. Some numerical results are presented in section 5 and a conclusion is given in section 6.

2. Discrete setting

In this section, we present the discretization involved in our method.

2.1. Time discretization

Let N be the number of time steps, $\Delta t = T/N$ and introduce $\varepsilon_j, \tilde{\varepsilon}_j, \Psi_j, \chi_j$ that stand respectively for the approximations of $\varepsilon(j\Delta t)$, $\tilde{\varepsilon}(j\Delta t)$, $\Psi(j\Delta t)$ and $\chi(j\Delta t)$ respectively. We denote in the following $\underline{\varepsilon} = (\varepsilon_j)_{0\leqslant j\leqslant N}$, $\underline{\tilde{\varepsilon}} = (\tilde{\varepsilon}_j)_{0\leqslant j\leqslant N}$, $\underline{\Psi} = (\Psi_j)_{0\leqslant j\leqslant N}$, $\underline{\chi} = (\chi_j)_{0\leqslant j\leqslant N}$.

For a given field $\varepsilon(t)$, a first numerical approximation of the final state $\Psi(T)$ is given by

$$\Psi(N\Delta t) \simeq \mathrm{e}^{-\mathrm{i}\Delta t(H_0-\mu\varepsilon_{N-1})}\mathrm{e}^{-\mathrm{i}\Delta t(H_0-\mu\varepsilon_{N-2})}\cdots\mathrm{e}^{-\mathrm{i}\Delta t(H_0-\mu\varepsilon_1)}\mathrm{e}^{-\mathrm{i}\Delta t(H_0-\mu\varepsilon_0)}\Psi_{\mathrm{init}}.$$

Note that in this approximation, we consider that the change in the Hamiltonian $H(t)$ can be neglected over a time step Δt. In practice the parameter Δt is chosen adequately to reproduce the oscillations of $H(t)$.

2.2. Toolkit discretization

In order to accelerate the computation, the toolkit method [1–3] proposes to approximate at each time step the field ε_j by a specific member ε_{r_j} of a predefined set $\{\varepsilon_r\}_{r=1,\ldots,m}$, with $m > 1$. Given arbitrary bounds $\varepsilon_{\min}, \varepsilon_{\max}$, we define

$$\varepsilon_r = \varepsilon_{\min} + (r-1)\Delta\varepsilon,$$

where $\Delta\varepsilon = \frac{1}{m-1}(\varepsilon_{\max} - \varepsilon_{\min})$ is the toolkit step.

To compute the evolution of the wavefunction over the $(j+1)$th time step, the propagator $\mathrm{e}^{-\mathrm{i}\Delta t(H_0-\mu\varepsilon_j)}$ is then replaced by the corresponding approximation $\Omega_{r_j} = \mathrm{e}^{-\mathrm{i}\Delta t(H_0-\mu\varepsilon_{r_j})}$, where $r_j = \mathrm{argmin}_{r=1,\ldots,m}\{|\varepsilon_j - \varepsilon_r|\}$.

Note that the precomputation of all exponentials $\{\Omega_r\}_{r=1,\ldots,m}$ is readily compensated since the total number of time steps Δt is usually (up to three order of magnitude) larger than the number of grid values for $\varepsilon(t)$.

2.3. Spectral decomposition

Let us now suppose that the operators H_0 and μ are discretized in a finite dimensional basis of size M. In this case, the precomputation of the exponentials Ω_r requires an offline effort

(i.e. in preparation to the operational phase) that scales as mM^3 and a storage of mM^2. The online phases on a time interval $[0, T = N\Delta t]$ require an effort that scales as NM^2.

Let us briefly discuss the computation of the propagated state over $[0, T]$. For each value ε_j, we denote by v_j^l and λ_j^l, the eigenmodes of $H_0 - \mu\varepsilon_j$ as

$$(H_0 - \mu\varepsilon_j)v_j^l = \lambda_j^l v_j^l, \qquad l = 1, \ldots, M, \quad j = 1, \ldots, m,$$

where m is the toolkit size. In this framework, the evolution of a state $\phi \in \mathbb{C}^M$ over $[t_j, t_{j+1} = t_j + \Delta t]$ with $\varepsilon(t) \approx \varepsilon_j$ is computed by

$$\mathrm{e}^{-\mathrm{i}\Delta t H(t_j)}\phi = \sum_{l=1}^{M} \langle v_j^l, \phi\rangle\, \mathrm{e}^{-\mathrm{i}\Delta t\lambda_j^l} v_j^l, \qquad l = 1, \ldots, M, \quad j = 1, \ldots, m.$$

3. Toolkit method and monotonic schemes

This section presents the structure of our optimization procedure.

3.1. Forward and backward propagations

Let us describe the kth iteration of our algorithm. Suppose that the piecewise constant field $\varepsilon^k(t)$ with amplitude values drawn from the electric-field toolkit $\{\varepsilon_r\}_{r=1,\ldots,m}$ is known. This field is integrated forward and backward in time, see equations (4)–(5), using the corresponding toolkit of propagators $\{\Omega_{r_j}\}_{j=0,\ldots,N-1}$ and their adjoints $\{(\Omega_{r_j})^*\}_{j=0,\ldots,N-1}$. In this way, the state $\Psi^k(t)$ and adjoint state $\chi^k(t)$ are computed at each time step over the time period $0 \leqslant t \leqslant T$. The evaluation of the quality of the field is given by the functional J. As described in the next sections, the electric field at each iteration is updated in such a way so as to maximize the functional. The new field is then discretized according to the toolkit field values, yielding the new trial field to compute $\Psi^{k+1}(t)$ and $\chi^{k+1}(t)$ with the toolkit $\{\Omega_r\}_{r=1,\ldots,m}$.

A direct implementation of the algorithms (7)–(10) involves a time discretization which may spoil the monotonic character, as we have shown below.

3.2. Example of a non-monotonic time-discretized scheme

We keep the notations introduced in section 2.1. A naive approach to discretize (7)–(10) is given by the following procedure:

Given initial control amplitudes $\underline{\varepsilon}^0, \underline{\tilde{\varepsilon}}^0$ and their associated state $\underline{\Psi}^0$ and adjoint state $\underline{\chi}^0$, suppose that for some $k \geqslant 1$, $\underline{\Psi}^k, \underline{\chi}^k, \underline{\varepsilon}^k, \underline{\tilde{\varepsilon}}^k$ have already been computed. Then $\underline{\Psi}^{k+1}, \underline{\chi}^{k+1}, \underline{\varepsilon}^{k+1}, \underline{\tilde{\varepsilon}}^{k+1}$ are computed as follows:

Step 1. Knowing $\Psi_0^{k+1} = \Psi_{\mathrm{init}}$, define Ψ_{j+1}^{k+1} from Ψ_j^{k+1} by

- Compute ε_j^{k+1} by

$$\varepsilon_j^{k+1} = (1 - \delta)\tilde{\varepsilon}_j^k - \frac{\delta}{\alpha}\,\mathrm{Im}\langle\chi_j^k|\mu|\Psi_j^{k+1}\rangle.$$

- Define $r_j^{k+1} = \mathrm{argmin}_{r=1,\ldots,m}\{|\varepsilon_j^{k+1} - \varepsilon_r|\}$.
- Compute Ψ_{j+1}^{k+1} by $\Psi_{j+1}^{k+1} = \Omega_{r_j^{k+1}}\Psi_j^{k+1}$.

Step 2. Knowing $\chi_N^{k+1} = O\Psi_N^{k+1}$, define χ_j^{k+1} from χ_{j+1}^{k+1} by

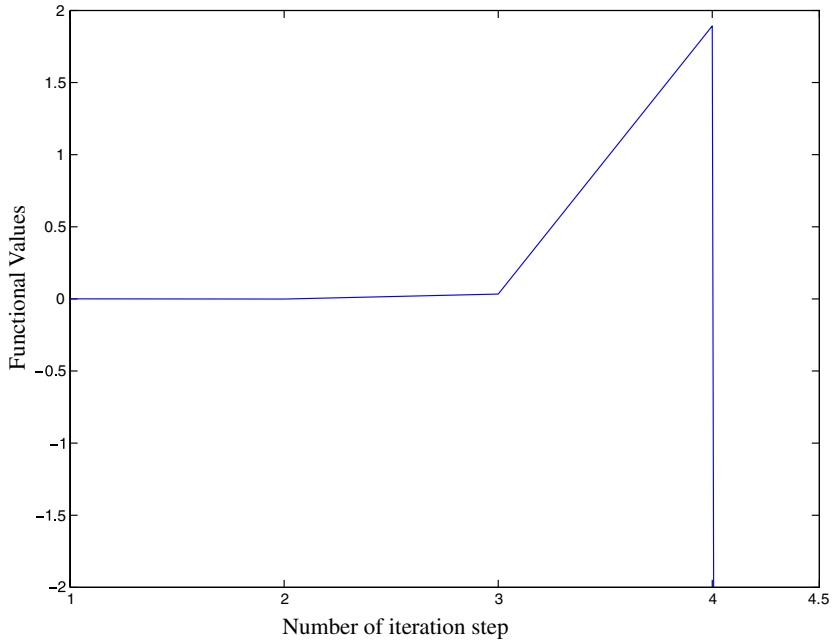

Figure 1. Unstable monotonic time-discretized scheme (in our simulation, $(\delta, \eta) = (1.75, 0.25)$, and $m = 800$). At the continuous level, the procedure should result in an increase of the functional value, while here the functional values are not improving during the iterations and even explode after the 4th iteration. The behaviour of our algorithm is similar for other choices of parameters $(\delta, \eta) \in [0, 2] \times [0, 2]$.

- Compute $\tilde{\varepsilon}_j^{k+1}$ by
$$\tilde{\varepsilon}_j^{k+1} = (1 - \eta)\varepsilon_j^{k+1} - \frac{\eta}{\alpha} \operatorname{Im}\langle \chi_{j+1}^{k+1} | \mu | \Psi_{j+1}^{k+1} \rangle.$$
- Define $\tilde{r}_j^{k+1} = \operatorname{argmin}_{r=1,\ldots,m} \{ |\tilde{\varepsilon}_j^{k+1} - \varepsilon_r| \}$.
- Compute χ_j^{k+1} by $\chi_j^{k+1} = \left(\Omega_{\tilde{r}_j^{k+1}}\right)^* \chi_{j+1}^{k+1}$.

Although this procedure corresponds to a direct discretization of (7)–(10), this scheme develops numerical instabilities, as shown in figure 1, so that the best field computed with this algorithm is the one obtained before numerical explosion, see figure 2.

For the numerical simulation, we choose a typical one-dimensional test system [7, 4] consisting of an excitation from the ground state to a certain target Morse potential of the O–H bond. For the numerical details concerning this test, we refer the reader to section 5.

4. Monotonic time-discretized scheme

We present an approach to discretize algorithms (7)–(10) so that they remain monotonic in the toolkit framework. To do this, we introduce the following time-discretizated version of the functional J (see equation (3)):

$$J_{\Delta t}(\varepsilon) = \langle \Psi_N | O | \Psi_N \rangle - \alpha \Delta t \sum_{j=0}^{N-1} \varepsilon_j^2.$$

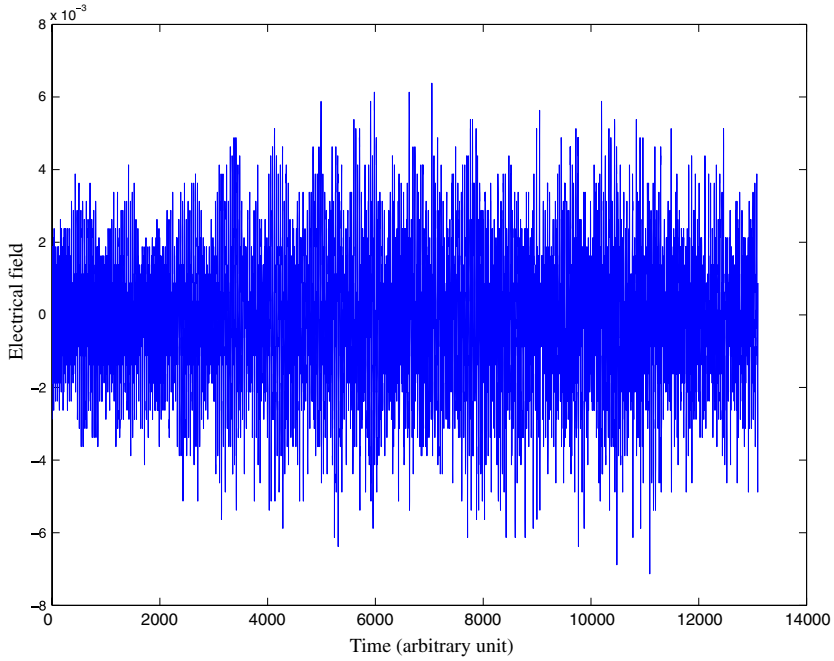

Figure 2. Optimized electric field obtained before numerical explosion (in our simulation, $(\delta, \eta) = (1.75, 0.25)$, and $m = 800$). The optimized electric field behaviour is similar for other choices of parameters $(\delta, \eta) \in [0, 2] \times [0, 2]$.

4.1. Preliminary

Assuming that another set of control amplitudes $\underline{\varepsilon'}$ is given, with associated state $\underline{\Psi'}$ and adjoint state $\underline{\chi'}$, we analyse the difference of the functionals. We have

$$J_{\Delta t}(\underline{\varepsilon'}) - J_{\Delta t}(\underline{\varepsilon}) = \langle \Psi'_N - \Psi_N | O | \Psi'_N - \Psi_N \rangle + 2\,\mathrm{Re}\langle \Psi'_N - \Psi_N | O | \Psi_N \rangle + \alpha \Delta t \sum_{j=0}^{N-1} \left(\varepsilon_j^2 - {\varepsilon'_j}^2 \right),$$

where the notation $\mathrm{Re}(z)$ is used to denote the real part of the complex number z. Focusing on $\langle \Psi'_N - \Psi_N | O | \Psi_N \rangle$, we find

$$\begin{aligned}
\langle \Psi'_N - \Psi_N | O | \Psi_N \rangle &= \langle \Psi'_N - \Psi_N, \chi_N \rangle \\
&= \sum_{j=0}^{N-1} \langle \Psi'_{j+1} - \Psi_{j+1}, \chi_{j+1} - \chi_j \rangle + \langle \Psi'_{j+1} - \Psi_{j+1} - \Psi'_j + \Psi_j, \chi_j \rangle \\
&= \sum_{j=0}^{N-1} \langle \Psi'_{j+1} - \Psi_{j+1}, (\mathrm{e}^{-\mathrm{i}\Delta t (H_0 - \mu \tilde{\varepsilon}_j)} - Id) \chi_j \rangle \\
&\quad + \sum_{j=0}^{N-1} \langle (Id - \mathrm{e}^{\mathrm{i}\Delta t (H_0 - \mu \varepsilon'_j)}) \Psi'_{j+1}, \chi_j \rangle - \sum_{j=0}^{N-1} \langle (Id - \mathrm{e}^{\mathrm{i}\Delta t (H_0 - \mu \varepsilon_j)}) \Psi_{j+1}, \chi_j \rangle
\end{aligned}$$

$$= \sum_{j=0}^{N-1} \langle (e^{i\Delta t(H_0-\mu\tilde{\varepsilon}_j)} e^{-i\Delta t(H_0-\mu\varepsilon'_j)} - Id)\Psi'_j, \chi_j \rangle$$
$$+ \sum_{j=0}^{N-1} \langle \Psi_{j+1}, (e^{-i\Delta t(H_0-\mu\varepsilon_j)} e^{i\Delta t(H_0-\mu\tilde{\varepsilon}_j)} - Id)\chi_{j+1} \rangle.$$

Finally we obtain the formula

$$J_{\Delta t}(\underline{\varepsilon'}) - J_{\Delta t}(\underline{\varepsilon}) = \langle \Psi'_N - \Psi_N | O | \Psi'_N - \Psi_N \rangle + \sum_{j=0}^{N-1} \phi_j^{\tilde{\varepsilon}}(\varepsilon') + \tilde{\phi}_j^{\varepsilon}(\tilde{\varepsilon}),$$

where

$$\phi_j^{\tilde{\varepsilon}}(\varepsilon') = 2\mathrm{Re}\langle (e^{i\Delta t(H_0-\mu\tilde{\varepsilon}_j)} e^{-i\Delta t(H_0-\mu\varepsilon'_j)} - Id)\Psi'_j, \chi_j \rangle + \alpha\Delta t((\tilde{\varepsilon}_j)^2 - (\varepsilon'_j)^2)$$
$$\tilde{\phi}_j^{\varepsilon}(\tilde{\varepsilon}) = 2\mathrm{Re}\langle \Psi_{j+1}, (e^{-i\Delta t(H_0-\mu\varepsilon_j)} e^{i\Delta t(H_0-\mu\tilde{\varepsilon}_j)} - Id)\chi_{j+1} \rangle + \alpha\Delta t((\varepsilon_j)^2 - (\tilde{\varepsilon}_j)^2).$$

This formula allows us to design schemes that remain monotonic after time discretization. To ensure monotonical increase towards the optimum (i.e. $J_{\Delta t}(\underline{\varepsilon'}) \geqslant J_{\Delta t}(\underline{\varepsilon})$), it is sufficient to find ε' such that

$$\forall j = 0, \ldots, N-1, \qquad \phi_j^{\tilde{\varepsilon}}(\varepsilon') \geqslant 0, \qquad \tilde{\phi}_j^{\varepsilon}(\tilde{\varepsilon}) \geqslant 0.$$

The strategy we choose is the following: given a field $\underline{\varepsilon}$, the values $\tilde{\varepsilon}_j$ are computed recursively with respect to j so that $\tilde{\phi}_j^{\varepsilon}(\tilde{\varepsilon})$ is positive (and maximized) at each time step. The same procedure is then applied to the term $\phi_j^{\tilde{\varepsilon}}(\varepsilon')$ to define ε', the updated value of ε.

4.2. Definition of the scheme

The previous part enables us to complete the description of the algorithm initiated in section 3.1.

4.2.1. Local optimization. We describe the computation of ε^{k+1}. Suppose that the sequence $(\tilde{r}_j^k)_{j=0,\ldots,N-1}$ and r_ℓ^{k+1}, with $\ell < j$ are known and define $\tau_j : \varepsilon_j^{k+1} \mapsto \phi_j^{\tilde{\varepsilon}}(\varepsilon^{k+1})$. The optimal choice of ε_j^{k+1} corresponds to the maximum of τ_j within the set of toolkit values $\{\varepsilon_r\}_{r=1,\ldots,m}$. To locate this point, we approximate τ_j by a second-order polynomial in a neighbourhood of $x = \varepsilon_{\tilde{r}_j^k}$ which can be obtained through the Taylor expansion,

$$\tau_j(x+h) = a_0 + a_1 h + a_2 h^2 + o(h^2).$$

Note that $\varepsilon_j^{k+1} = \varepsilon_{\tilde{r}_j^k}$ cancels τ_j, hence $a_0 = 0$.

Then, the coefficients a_1 and a_2 can be computed using $\tau_j(x+\Delta\varepsilon)$ and $\tau_j(x-\Delta\varepsilon)$, where $\Delta\varepsilon$ is the toolkit step, see section 2.2. Indeed, we have

$$\begin{cases} a_1 = \dfrac{\tau_j(x+\Delta\varepsilon) - \tau_j(x-\Delta\varepsilon)}{2\Delta\varepsilon} \\ a_2 = \dfrac{\tau_j(x+\Delta\varepsilon) + \tau_j(x-\Delta\varepsilon)}{2(\Delta\varepsilon)^2}. \end{cases} \tag{11}$$

The maximum of this polynomial in h is achieved for

$$h_j^{\star k+1} = -\frac{a_1}{2a_2}, \tag{12}$$

which suggests to define r_j^{k+1} as the index of the toolkit value that is the closest to $\varepsilon_{\tilde{r}_j^k} + h_j^{\star k+1}$. In order to guarantee the monotonicity of our algorithm, we test the positivity of $\tau_j(\varepsilon_{r_j^{k+1}})$

before the computation of Ψ_{j+1}^{k+1}. If $\tau_j(\varepsilon_{r_j^{k+1}}) < 0$, the index r_j^{k+1} is redefined by $r_j^{k+1} = \tilde{r}_j^k$ which leads to $\tau_j(\varepsilon_{r_j^{k+1}}) = 0$. The field index update is summarized by the formula

$$r_j^{k+1} = \begin{cases} \operatorname{argmin}_{r=1,\dots,m}\left\{\left|\tilde{\varepsilon}_j^k + h_j^{\star k+1} - \varepsilon_r\right|\right\}, & \text{if} \quad \tau_j(\varepsilon_{r_j^{k+1}}) \geqslant 0 \\ \tilde{r}_j^k, & \text{otherwise.} \end{cases} \tag{13}$$

In the same way, $\tilde{r}_j^{k+1}$ is defined by

$$\tilde{r}_j^{k+1} = \begin{cases} \operatorname{argmin}_{r=1,\dots,m}\left\{\left|\varepsilon_j^{k+1} + g_j^{\star k+1} - \varepsilon_r\right|\right\}, & \text{if} \quad \tau_j(\varepsilon_{\tilde{r}_j^{k+1}}) \geqslant 0 \\ r_j^{k+1}, & \text{otherwise,} \end{cases} \tag{14}$$

where $(g_j^\star)^{k+1}$ is obtained in the same way as $(h_j^\star)^{k+1}$.

Remark 4.1. In order to improve the efficiency of the algorithm, one can approximate τ_j using additional values, e.g. by computing, for a given integer n, $\tau_j\left(\tilde{\varepsilon}_j^k - \Delta\varepsilon\right)$, $\tau_j\left(\tilde{\varepsilon}_j^k + \Delta\varepsilon\right)$, $\tau_j\left(\tilde{\varepsilon}_j^k - 2\Delta\varepsilon\right)$, $\tau_j\left(\tilde{\varepsilon}_j^k + 2\Delta\varepsilon\right), \dots, \tau_j\left(\tilde{\varepsilon}_j^k - n\Delta\varepsilon\right)$, $\tau_j\left(\tilde{\varepsilon}_j^k + n\Delta\varepsilon\right)$ and then find the maximum of the polynomial that best fits this sample.

Remark 4.2. Note that the computations of the coefficients a_1 and a_2 take advantage of the toolkit approach since it only uses matrices $\{\Omega_r\}_{r=1,\dots,m}$; as such the additional cost is of the same order of magnitude as the cost of advancing one time step.

4.2.2. Algorithm. We are now in a position to give the definition of our algorithm. Given initial control amplitudes $\underline{\varepsilon}^0, \underline{\tilde{\varepsilon}}^0$ and their associated state $\underline{\Psi}^0$ and adjoint state $\underline{\chi}^0$, suppose that for some $k \geqslant 1$, $\underline{\Psi}^k, \underline{\chi}^k, \underline{\varepsilon}^k, \underline{\tilde{\varepsilon}}^k$ have already been computed. The iterated quantities $\underline{\Psi}^{k+1}, \underline{\chi}^{k+1}, \underline{\varepsilon}^{k+1}, \underline{\tilde{\varepsilon}}^{k+1}$ are defined as follows:

$$\begin{cases} \Psi_{j+1}^{k+1} = \Omega_{r_j^{k+1}} \Psi_j^{k+1} \\ \Psi_0^{k+1} = \Psi_{\text{init}}, \end{cases} \tag{15}$$

where r_j^{k+1} is defined by (13),

$$\begin{cases} \chi_j^{k+1} = (\Omega_{\tilde{r}_j^{k+1}})^* \chi_{j+1}^{k+1} \\ \chi_N^{k+1} = O\Psi_N^{k+1}, \end{cases} \tag{16}$$

where $\tilde{r}_j^{k+1}$ is defined by (14).

5. Numerical results

In order to confirm the theoretical result analysed in section 4, we choose a typical one-dimensional test system [4, 7] consisting of the O–H-bond that vibrates in a Morse-type potential $V(x) = D_0((\mathrm{e}^{-\beta(x-x_0)} - 1)^2 - 1)$, with $D_0 = 0.1994$, $\beta = 1.189$ and $x_0 = 1.821$. The dipole moment function is $\mu(x) = \mu_0 x\, \mathrm{e}^{-x/x^*}$ with $\mu_0 = 3.088\,4041$, $x^* = 0.6$. The goal is to localize the wave packet at a given location x'; this is expressed via the observable $O(x) = \frac{\gamma_0}{\sqrt{\pi}}\, \mathrm{e}^{-\gamma_0^2(x-x')^2}$ through the requirement that $\langle\Psi(T)|O|\Psi(T)\rangle$ is maximized (γ_0 and x' are chosen to be 25.0 and 2.5 respectively). The final time is $T = 131\,000$ and the time step is $\mathrm{d}T = 10$. The input field is taken as $\varepsilon^0(t) = 0$ and the penalty factor is $\alpha = 1$.

Figure 3 shows the evolution of the values of the functional versus the number of iteration steps for different parameter values m of the toolkit's size. The numerical calculation confirms

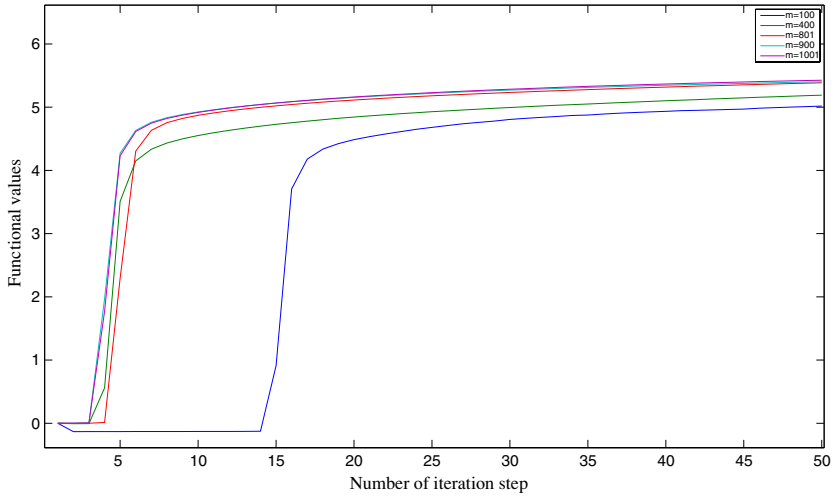

Figure 3. Evolution of the functional J for different parameter values m. It is a characteristic of the monotonic schemes to obtain good quality after few iteration steps: the first steps give the major contributions to obtain almost 80% of its maximum value of the optimized objective functional. All curves have the same asymptotic behavior. Working with $m = 800$ is an efficient compromise between numerical accuracy and small computational time.

the theoretical result of section 4 as each additional iteration step monotonically improves the previous iteration step by adding a positive term.

We set the initial field to zero, which is almost a critical point of the functional; as such, when zero is a toolkit value (i.e. for odd m) the field may not change; in contrast, for even m the field will need an iteration to take admissible toolkit values (and as such the first iteration may not be monotonic) but this small adjustment will force it to leave the critical point. Thus the overall convergence will be better for even m than for odd m.

6. Conclusion

In this communication, we propose a numerical improvement of the 'toolkit' method which preserves the monotonicity of the optimization algorithms used to find the best quantum control field. The properties of the new algorithm are analysed theoretically in section 4, and numerical test in section 5 confirms the theoretical result. The method accelerates the computation and can be used to obtain an initial assumption when considering more precise or higher order methods.

Acknowledgments

This work is partially supported by the French ANR C-QUID project, INRIA Rocquencourt (MicMac project) and PICS-NSF program 'Manipulation and identification of quantum phenomena'.

References

[1] Balint-Kurti G G, Manby F R, Ren Q, Artamonov M, Ho T and Rabitz H 2005 Quantum control of molecular motion including electronic polarization effects with a two-stage toolkit *J. Chem. Phys.* **122** 084–110

[2] Yip F L, Mazziotti D A and Rabitz H 2003 A local-time algorithm for achieving quantum control *J. Phys. Chem.* A **107** 7264–9
[3] Yip F, Mazziotti D and Rabitz H 2003 A propagation toolkit to design quantum control *J. Chem. Phys.* **118** 8168–72
[4] Maday Y and Turinici G 2003 New formulations of monotonically convergent quantum control algorithms *J. Chem. Phys.* **118** 8191–6
[5] Schirmer S, Girardeau M and Leahy J 2000 Efficient algorithm for optimal control of mixed-state quantum systems *Phys. Rev.* A **61** 012101
[6] Hornung T, Motzkus M and de Vivie-Riedle R 2001 Adapting optimal control theory and using learning loops to provide experimentally feasible shaping mask patterns *J. Chem. Phys.* **115** 3105–11
[7] Zhu W and Rabitz H 1998 A rapid monotonically convergent iteration algorithm for quantum optimal control over the expectation value of a positive definite operator *J. Chem. Phys.* **109** 385–91
[8] Tannor D, Kazakov V and Orlov V 1992 Control of photochemical branching: Novel procedures for finding optimal pulses and global upper bounds *Time Dependent Quantum Molecular Dynamics* ed J Broeckhove and L Lathouwers (New York: Plenum) pp 347–60